Integration of Gas Enhanced Oil Recovery in Multiphase Fermentations for the Microbial Production of Fuels and Chemicals

Pedraza-de la Cuesta, Susana; Keijzers, Lore; van der Wielen, Luuk A.M.; Cuellar Soares, Maria

DOI
10.1002/biot.201700478

Publication date
2018

Document Version
Final published version

Published in
Biotechnology Journal

Citation (APA)
Pedraza-de la Cuesta, S., Keijzers, L., van der Wielen, L. A. M., & Cuellar Soares, M. (2018). Integration of Gas Enhanced Oil Recovery in Multiphase Fermentations for the Microbial Production of Fuels and Chemicals. *Biotechnology Journal*, *13*(4), Article 1700478. https://doi.org/10.1002/biot.201700478

RESEARCH ARTICLE

Bioprocess Engineering

Biotechnology Journal

www.biotechnology-journal.com

Integration of Gas Enhanced Oil Recovery in Multiphase Fermentations for the Microbial Production of Fuels and Chemicals

*Susana Pedraza-de la Cuesta, Lore Keijzers, Luuk A. M. van der Wielen, and Maria C. Cuellar**

In multiphase fermentations where the product forms a second liquid phase or where solvents are added for product extraction, turbulent conditions disperse the oil phase as droplets. Surface-active components (SACs) present in the fermentation broth can stabilize the product droplets thus forming an emulsion. Breaking this emulsion increases process complexity and consequently the production cost. In previous works, it has been proposed to promote demulsification of oil/supernatant emulsions in an off-line batch bubble column operating at low gas flow rate. The aim of this study is to test the performance of this recovery method integrated to a fermentation, allowing for continuous removal of the oil phase. A 500 mL bubble column is successfully integrated with a 2 L reactor during 24 h without affecting cell growth or cell viability. However, higher levels of surfactants and emulsion stability are measured in the integrated system compared to a base case, reducing its capacity for oil recovery. This is related to release of SACs due to cellular stress when circulating through the recovery column. Therefore, it is concluded that the gas bubble-induced oil recovery method allows for oil separation and cell recycling without compromising fermentation performance; however, tuning of the column parameters considering increased levels of SACs due to cellular stress is required for improving oil recovery.

1. Introduction

Recent advances in strain development have enabled the production of extracellular hydrocarbons such as alkanes and sesquiterpenes in microbial fermentations.[1] The immiscible product, with a lower density than the aqueous medium, forms an oil phase that readily separates from the fermentation broth (**Figure 1**A). This opens the opportunity of integrating a low-cost recovery operation such as settling or hydrocyclone into the fermentation allowing for cell recycling and process cost reduction. In reality, however, turbulent mixing conditions in the reactor and the presence of surface-active components (SACs) in the fermentation broth (e.g., salts, glycolipids, proteins, cells, and cells debris) disperse the product phase forming an emulsion of small stable oil droplets (Figure 1B). Reported recovery methods at large scale require using costly surfactants and changes of temperature,[2] which might compromise the purity specifications,[3] increase costs, and prevent cellular recycling by affecting cell viability.[4] Although the need for a low-cost demulsification process might be more relevant in the case of applications with tight economic margins such as biofuels, the problem of recovery of microbial emulsions is not new. Solvents are widely used for product extraction in fermentations and bioconversions to enhance product recovery, avoid toxicity problems, or reduce product evaporation.[5,6] The dispersion of solvent containing product leads to similar emulsification problems as encountered in microbial fermentations of extracellular hydrophobic hydrocarbons.[7] Technologies such as gravity settling,[8] and membranes[9] have been described for organic phase recovery during the bioconversion.

Recently a gas-enhanced oil recovery (GEOR) technology has been proposed as an alternative to recover emulsified fermentation products.[10] This technology consists of promoting the coalescence of oil droplets forming a continuous oil layer by passing gas bubbles through an emulsion. By adjusting bubble size, number of bubbles, and aspect ratio, GEOR was proven to be effective in diverse emulsions of hexadecane in an aqueous

S. Pedraza-de la Cuesta, L. Keijzers, Prof. L. A. M. van der Wielen, Dr. M. C. Cuellar
Department of Biotechnology
Delft University of Technology
van der Maasweg 9, 2629HZ Delft, The Netherlands
E-mail: m.c.cuellar@tudelft.nl

Prof. L. A. M. van der Wielen
Bernal Institute
University of Limerick
Castletroy, Limerick, Ireland

Prof. L. A. M. van der Wielen
BE-Basic Foundation
Mijnbouwstraat 120, 2628 RX Delft, The Netherlands

DOI: 10.1002/biot.201700478

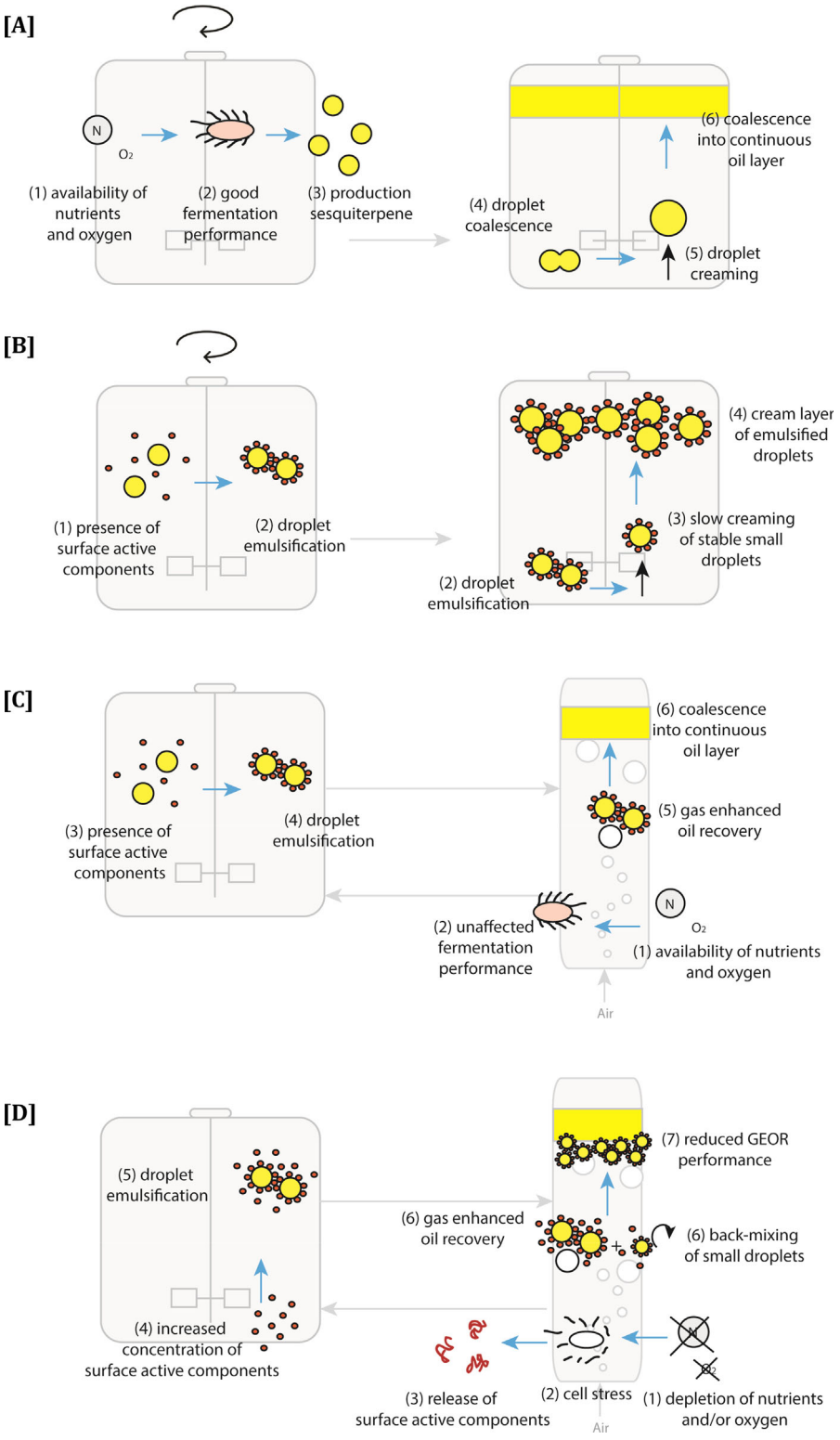

Figure 1. Representation of production (left) and recovery subprocesses (right) taking place in different scenarios of multiphasic fermentations: (A) ideal scenario if no surface active components (SACs) are present and a continuous oil layer is formed after the fermentation; (B) scenario in which emulsification takes places preventing direct oil phase recovery after fermentation; (C) illustration of an integration of a GEOR column using gas bubbles at mild mixing conditions to aid demulsification, while allowing for cell recycle; (D) mild mixing conditions required for droplet separation could lead to cellular stress and release of SACs reducing recovery efficiency.

mixture of water and the yeast *Saccharomyces cerevisiae*. It remains unknown how the technology would perform in an actual fermentation broth where SACs can affect the stability of the emulsion.

This work concerns the implementation of GEOR in the recovery of oil from microbial emulsions by presenting an integrated bioreactor-GEOR system. In this integrated configuration, the fermentation broth containing a dispersion of oil droplets is circulated through a GEOR column. In the column, the oil/water separation takes place with the aid of gas bubbles, and the oil depleted broth is transferred back into the reactor (Figure 1C). The main advantage of GEOR lies in reducing the number of separation steps, while avoiding the use of costly chemicals. In addition, GEOR might offer several advantages when continuously integrated into a fermentation, such as: i) cell recycle; (ii) prevention of further stabilization of the emulsion over time; and (iii) avoiding oxygen transfer problems[11] in case of excessive accumulation of oil in the bioreactor. On the other hand, GEOR is typically performed at low gas flow rates and mild mixing conditions. This poses some operational and design challenges, namely related to possible oxygen and nutrient limitation occurring in the recovery compartment (Figure 1D).

The aim of this work is to study the feasibility of integrating a GEOR column to a bioreactor, with especial focus on fermentation performance, emulsion behavior, and oil recovery.

2. Theoretical Background

The integrated process presented in this work consists of a well-mixed fermentation compartment operating in fed-batch mode, connected to an external bubble column which typically operates at milder mixing conditions to promote oil recovery[10] (**Figure 2**B). The main subprocesses taking place in the separation column are: i) circulation of the broth through the

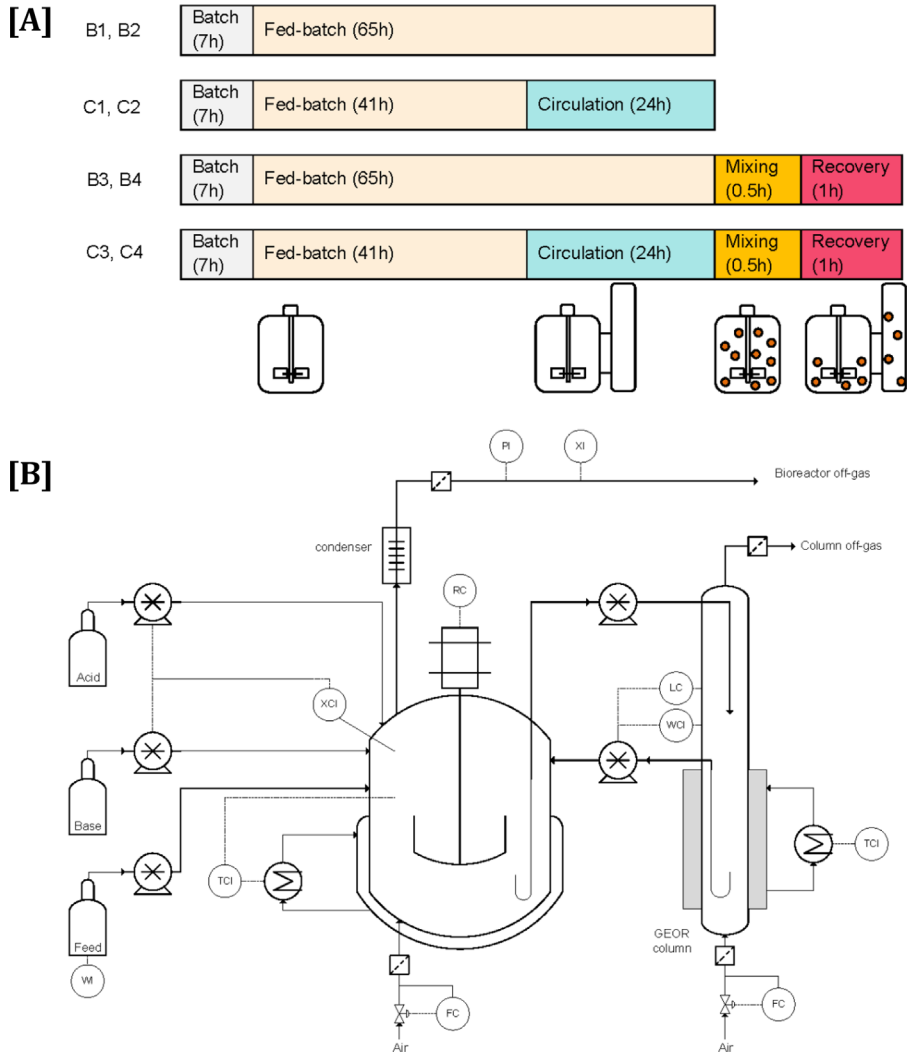

Figure 2. A) Overview fermentation stages in the different experiments. B) Schematic representation of the integrated system. P-pressure; X-composition; R-agitation speed; T-temperature; W-weight; F-mass flow; L-level; I-indicator; C-controller.

column; ii) mixing of the bulk liquid due to bubbles; iii) creaming of the oil droplets due to difference of density; and iv) coalescence of separated oil droplets into a clear oil layer on the top part of the column aided by the gas bubbles. Although the exact mechanism(s) whereby the separated oil droplets coalesce into a clear oil layer are not yet understood, the degree of oil recovery in the column can be estimated by performing a regime analysis as the one presented in Ref. [12].

Separation of oil droplets from the continuous phase takes place when the time required for a droplet to rise (addressed in this work as creaming characteristic time, τ_{cream}) is shorter than the time required to mix the liquid in the column (τ_{mix}):

$$\tau_{cream} < \tau_{mix} \quad (1)$$

In addition, the residence time of the bulk liquid in the column (τ_{res}) should be larger than the creaming time in order to allow droplets to stay in the column:

$$\tau_{cream} < \tau_{res} \quad (2)$$

The characteristic time for mixing in columns with aspect ratio higher than three depends on the column aspect ratio and the superficial gas velocity at which the column operates (v_{GS}).[13]

$$\tau_{mix}^{column} = 1.496 \cdot \left(\frac{D_{column}{}^2}{g \cdot v_{GS}}\right)^{\frac{1}{3}} \cdot \left(\frac{H_{column}}{D_{column}}\right)^2 \quad (3)$$

The residence time of the fermentation broth in the column (τ_{res}) depends on the bulk liquid flow (F_L) and the volume of liquid in the column (V_{col}):

$$\tau_{res} = V_{column}/F_L \quad (4)$$

Finally, the characteristic time for creaming (Eq. (5)) depends of the column height (H_{column}), and the droplet velocity (v_d), which at the same time depends on the density difference between the oil (ρ_{oil}) and the continuous phase (ρ_L), the droplet size diameter (d_d), gravitational acceleration (g), and the drag coefficient (C_D) (Eq. (6)).

$$\tau_{cream} = H_{column}/v_d \quad (5)$$

$$v_d = \sqrt{\frac{4 \cdot g \cdot (\rho_L - \rho_{oil}) \cdot d_d}{3 \cdot C_D \cdot \rho_L}} \quad (6)$$

As previously described in Ref. [12], the oil droplets dispersed in the fermentation compartment due to the turbulent conditions range between d_{min} (Eq. (7)) and d_{max} (Eq. (8)) depending on the o/w interfacial tension (σ_{oil}), the continuous phase density (ρ_L) and viscosity (η_w), and the volumetric power input (e_v), which depends on the stirring rate (N), the aeration rate (F_G), the diameter of the impeller ($D_{impeller}$), and the bioreactor working volume (V_R) (Eq. (9)).

$$d_{min}\left(\frac{\sigma_{oil}^{1.38} \cdot \left(10^{-28}\right)^{0.46} \cdot \rho_L^{0.05}}{0.072 \cdot \eta_w \cdot e_v^{0.89}}\right)^{\frac{1}{3.11}} \quad (7)$$

$$d_{max} = \left(\frac{\sigma_{oil}^3}{\rho_L \cdot e_v^2}\right)^{\frac{1}{5}} \quad (8)$$

$$e_v^{reactor} = \left(5.5 \cdot \rho_L \cdot N^3 \cdot D_{impeller}^5\right)\left(1 - \frac{9.9 \cdot F_G \cdot N^{0.25}}{D_{impeller}^5}\right)\frac{I}{V_R} \quad (9)$$

Considering Eqs. (1)–(9) it is possible to find an operational window where column geometry, column aeration rate, and bulk liquid flow allow for droplet separation. However, when designing the recovery compartment, not only hydrodynamics are important but also cellular responses and their effect on productivity and recovery. Although mild mixing conditions are required in the column to promote oil creaming[10] this regime could lead to cellular stress caused by oxygen or nutrients limitation (Figure 1). The possible consequences are diverse, such as release of SACs that include proteins,[14] polysaccharides,[15] carboxylic acids[16], to the increase of cell membrane hydrophobicity, loss of productivity and viability.[14] These cellular responses could have an effect in the oil emulsification; either by reducing droplet coalescence,[17] or by stabilizing the o/w interface.[18,19] In addition, the accumulation of oil in the column could increase bubble coalescence and the medium apparent viscosity contributing to oxygen limitation.[11]

2.1. Aim and Approach

The aim of this work is to study the effect of broth circulation through a GEOR column on fermentation performance and oil recovery. Model fermentations with wild-type *Escherichia coli* were performed, and hexadecane was eventually added to mimic microbial oil production and/or solvent extraction. Hexadecane was chosen due to its biocompatibility (log P of 8.8),[20] its similarity in number of carbons compared to commercial microbial oils like sesquiterpenes (C_{15}), and the availability of GEOR data with this organic phase.[10] This approach allows to fix the oil concentration regardless of fermentation performance. Consequently, fermentation performance and degree of oil recovery can be decoupled.

Four sets of experiments with duplicates were performed (Figure 2A): a base case consisting of a fed-batch fermentation in a reactor vessel (B1, B2); a fed-batch fermentation in a reactor vessel circulating part of the broth through a GEOR column for 24 h (C1, C2); addition of 10% w/w of hexadecane to a base case fermentation and recovering the oil by circulating the dispersion through the GEOR column for 1 h (B3, B4); and addition of 10% w/w of hexadecane to a fermentation similar to C1 and C2, and recovering the oil by circulating the dispersion through the GEOR column for 1 h (C3, C4).

In order to study how the circulation of broth through the column affects the fermentation performance, cell growth, cell viability, and level of SACs in the integrated system (C1–C4) were compared to the base case (B1–B4). Proteins have been shown to play an important role in stabilization of hexadecane microbial emulsions,[10,21] and consequently, they have been chosen as reference component for measuring levels of SACs. In order to discard any possible source of cellular stress other than the circulation though the GEOR column, feed rate, aeration, and

stirrer speed were chosen such to avoid oxygen limitation in the main vessel.

As it is shown in Figure 1D, the cellular stress responses to the circulation of broth through the recovery column can have an effect in the emulsion stability. Consequently, the extent of oil recovery can be reduced. The impact of eventual cell stress responses in separation performance was evaluated by comparing the oil hold-up in the GEOR column of the base case (B3, B4) and circulation case (C3, C4).

3. Experimental Section

3.1. Experimental Set Up

The experimental set up consisted of a 2 L jacketed reactor (Applikon, the Netherlands), working in fed batch mode under glucose limitation connected by a Masterflex peristaltic pump (Cole Parmer, USA) and Masterflex Tygon Fuel & Lubricant tubing L/S 17 to a 500 mL glass-column as indicated in Figure 2.

The custom-made column of 37 mm inner diameter (40 mm outer diameter) and 600 mm height was aerated at 0.1 cm s^{-1} through a stainless-steel bottom plate with a single nozzle of 0.3 mm diameter and an off-gas outlet located at the top. The nozzle and aeration rate conditions in the column were selected based on the results reported by Ref. [8] to allow the formation of phase gradient in the column.

In order to avoid excessive circulation of bubbles from the bioreactor vessel to the recovery column, the extreme of the outlet port was designed as a u-tube. The cell broth was circulated back to the fermentation vessel by a second Masterflex peristaltic pump (Cole Parmer) activated either by a level sensor (C1 and C2) or by a weight sensor (C3 and C4). The temperature in the column was maintained at 35 °C by an external heating coil, connected to a cryostat (Lauda, USA), and tubes connecting the two compartments were insulated to avoid heat loss.

3.2. Strain, Pre-Culture Medium, and Fermentation Medium

The strain used in this work is a *E. coli* K12 (MG1655) obtained from The Netherlands Culture Collection of Bacteria (Utrecht, the Netherlands). A total of 0.5 mL of stock culture stored at −80 °C in Luria-Bertani (LB) medium containing 15% v/v glycerol, were inoculated in 100 mL of sterile synthetic medium (SM)[22] supplemented with 15 g L^{-1} $C_6H_{12}O_6 \cdot H_2O$, and 0.0045 g L^{-1} Thiamine · HCl. Precultures were incubated overnight (≈14 h) in 300 mL shake flasks at 35 °C and 200 rpm in a rotary shaker (Sartorius Stedim Biotech S.A., France), and inoculated in 900 mL of sterile fermentation medium following the composition as reported in Ref. [23] using 5 g L^{-1} $C_6H_{12}O_6 \cdot H_2O$ as carbon source and 0.1 mL EROL DF 7911 K (PMC Ouvrie, France) as antifoaming agent.

3.3. Fed-Batch Fermentation

Fermentations were performed at an aeration rate of 1.5 nL min^{-1} controlled by a mass flow controller (Brooks, USA), and stirred with a 6-blade Rushton impeller of 45 mm diameter at speed of 1000 rpm. For fermentations B3, B4, C3, and C4 stirring speed was increased to 1200 rpm during the fed-batch phase in order to ensure a dissolved oxygen tension (DOT) above 20%; the temperature was set to 35 °C and the pH was maintained at 6.5 by adding acid (2M H_2SO_4) and base (NH_4OH 25% v/v). Fermentation settings were controlled by a ADI-1030 controller (Applikon). Foam was controlled by manual addition of an aqueous solution of 10% v/v antifoam Erol-DF7911K (PMC Ouvrie) up to a maximum of 30 g.

After ≈7.2 h of fermentation, glucose was consumed and the DOT increased indicating the end of the batch phase. At that point, a glucose solution containing 700 g L^{-1} $C_6H_{12}O_6 \cdot H_2O$, 20 g L^{-1} $MgSO_4 \cdot 7H_2O$, 0.045 g L^{-1} Thiamine · HCl, and the same trace metal concentration as in the batch medium, was fed into the bioreactor using a Masterflex peristaltic pump (Cole Parmer). In fermentations B1, B2, C1, C2, different feed mass flow rates between 5 and 10 g h^{-1} were chosen to test the validity of the model at different conditions. Experiments B3, B4, C3, C4 were performed at a constant feed rate of 7 g-solution h^{-1}. These feeding conditions were maintained throughout the experiments including circulation and recovery periods.

3.3.1. Circulation Period (C1–C4)

After 48 h from the beginning of the fermentation, the broth was circulated in fermentations C1–C4 through the recovery column for a period of 24 h at a mass flow of 3.16 g s^{-1} with a Masterflex pump and Tygon 17′ tubings (Masterflex), keeping a column working volume of 350 mL, and providing a liquid residence time one order of magnitude higher than the expected creaming time.

3.3.2. Recovery Period (B3, B4, C3, and C4)

After 72 h of fermentation 10.0 ± 0.3% w/w of hexadecane (Sigma–Aldrich) colored with oil red-O dye (Sigma–Aldrich) was added to the reactor in fermentations B3, B4, C3, and C4. In fermentations C3 and C4, all the broth was transferred back to the reactor vessel prior to the addition of oil. After mixing the oil for 30 min, the dispersion was circulated through the GEOR column for 1 h, and pictures of the top of the column (equivalent to a picture area of 20 × 40 mm) were taken to evaluate the degree of oil recovery. The conditions in the reactor vessel and column, including feed rate, were the same as in the circulation period.

3.4. On-Line Analyses

DOT was measured by a dissolved oxygen sensor (Applikon; Mettler Toledo, the Netherlands). The CO_2 and O_2 concentrations in the bioreactor off-gas and in pressurized air were analyzed by a Rosemount NGA-2000 gas analyzer (Fisher Rosemount, Germany). pH was measured by a pH sensor (Applikon). Temperature was measured with a temperature sensor (Applikon). Feed rate was continuously monitored with a

balance (Mettler Toledo). DOT, concentrations of CO_2 and O_2 in the off gas and in pressurized air, pH, temperature, and feed weight were continuously recorded with a MFCS/Win 2.1 software (Sartorius Stedim Biotech S.A.).

3.5. Off-Line Analyses

3.5.1. Optical Density and Cell Dry Weight

Optical density of samples was measured in a spectrophotometer (Biochrom) at 600 nm. A total of 1.5 mL microcentrifuge tubes containing 1 mL of broth were set in a centrifuge (Heraeus, Biofuge Pico) at 13 000 rpm for 10 min. After discarding the supernatant, the tubes containing the cell pellet were dried in an oven (Heraeus instruments) at 70 °C for 48 h.

3.5.2. HPLC, TOC, and Protein Analysis

Supernatant was separated from the cells in a centrifuge (Heraeus instruments, Stratos) at 17 000 rpm for 20 min at 4 °C and filtered with a disk filter (Whatman) of 0.45 µm in fermentations B1, B2, C1, and C2 and a disk filter (Whatman) of 0.22 µm in fermentations B3, B4, C3, and C4.

Extracellular amount of residual glucose, ethanol, glycerol, and acetate were determined in supernatant by high-performance liquid chromatography (HPLC) as described in Ref. [24].

The total amount of organic carbon (TOC) in broth and supernatant was analyzed at the end of the fermentation (except in B3 and C3) with a Total Carbon (TC) analyzer (Shimadzu). Extracellular protein concentration in the supernatant was determined using a Bradford Protein Assay Kit (Thermo Scientific). Protein concentrations for circulation and non-circulation experiments were statistically compared by a two-tailed *t*-test assuming homoscedasticity.

3.5.3. Cell Viability

The concentration of colony forming units (CFU) in the sample was obtained by plating cells on sterile LB medium plates. Samples were diluted with sterile SM medium to ca. 10 CFU, 100 CFU, and 1000 CFU per plate. The plates were incubated for 24 h in an incubator (Heraeus instruments) at 30 °C after which the colonies were counted. Results for circulation and non-circulation experiments were statistically compared by a two-tailed *t*-test assuming homoscedasticity.

3.5.4. Oil Recovery: Experimental and Theoretical Values

Pictures of the top of the column were processed in Adobe Photoshop CS6, selecting and area of 20 × 20 mm (10 mm radius from the center of the column) and cropping the rest of the picture. The selected area was processed with the software ImageJ 1.47, characterizing number of droplets (N_i), droplet size distribution (d_i), and droplet area (A_i). The total area of droplets ($A_{oil,\ droplets}$) was compared to the total area of the picture (A_{20x20}) to estimate the oil hold-up, ε_{oil}:

$$\varepsilon_{oil} = \frac{A_{oil,droplets}}{A_{20\times 20}} \tag{10}$$

Under the assumption that this hold-up remained constant in the top of the column, the percentage of recovery was then estimated by comparing the volume of oil in the top of the column with the total volume of oil added in the experiment ($V_{oil,\ TOTAL}$):

$$\text{Recovery}(\%) = \frac{\varepsilon_{oil} \cdot A_{20\times 40} \cdot \pi \cdot D_{col}}{4 \cdot V_{oil,TOTAL}} \cdot 100 \tag{11}$$

With $A_{20\times 40}$ the picture area of the top of the column and D_{col} the column diameter. In addition, a theoretical oil droplet size distribution was calculated assuming a normal distribution between theoretical d_{min} and d_{max} (Eqs. (7) and (8), 0.04 and 1.55 mm, respectively) with a standard deviation equal to three times half of the range. For such droplet size distribution, the volume of oil accumulated in the column ($V_{oil,\ theoretical}$) when the droplets of sizes between d_i and d_{max} cream to the top section of the column is

$$V_{oil,theoretical} = \sum_{i}^{i=max} \frac{d_i^3}{6} \cdot \pi \cdot N_i \tag{12}$$

where N_i is the number of droplets of diameter d_i. The theoretical recovery percentage then becomes:

$$\text{Recovery}_{theoretical}\ (\%) = \frac{V_{oil,theoretical}}{V_{oil,TOTAL}} \cdot 100 \tag{13}$$

Note that when $d_i = d_{min}$ the theoretical recovery would be 100%, while if $d_i = d_{max}$, the theoretical recovery would be near 0%. Theoretical recovery values were estimated for a varying threshold of minimum droplet size being able to cream in the column (**Figure 5**C).

3.6. Fermentation Model and Carbon Balance

A model was developed to predict the cell and CO_2 fermentation profiles in the fed-batch phase. The mass balances of cells, substrate (glucose), and CO_2 in the reactor at constant feed rate are

$$dM_X(t)/dt = \mu(t) \cdot M_X(t) \tag{14}$$

$$dM_S(t)/dt = F_S + q_S(t) \cdot M_X(t) = 0 \tag{15}$$

$$dM_C(t)/dt = q_C(t) \cdot M_X(t) \tag{16}$$

For the substrate balance (Eq. (15)), a pseudo-steady state was assumed ($dM_S/dt \approx 0$) as glucose accumulation in the reactor during the carbon-limited fed-batch phase was negligible. The

specific rates of glucose consumption and CO_2 production are given by their respective Herbert–Pirt relations:

$$q_S(t) = \frac{1}{Y_{X/S}} \cdot \mu(t) - m_S \tag{17}$$

$$q_C(t) = \frac{Y_{C/S}}{Y_{X/S}} \cdot \mu(t) - m_{CO_2} \tag{18}$$

Combining Eqs. (14), (15), and (17), and Eqs. (16) and (18), the resulting cell-growth rate and CO_2 production rates are

$$R_X = dM_X(t)/dt = \mu(t) \cdot M_X(t) = F_S - m_S \cdot M_X(t) \cdot Y_{X/S} \tag{19}$$

$$R_C = dM_C(t)/dt = \frac{Y_{C/S}}{Y_{X/S}} \cdot \mu(t) \cdot M_X(t) + m_{CO_2} \cdot M_X(t) \tag{20}$$

The total cell mass profile (Eq. (17)) was obtained integrating Eq. (19). M_{X0} and t_0 represent the mass of cells and the fermentation time at beginning of the fed-batch phase.

$$M_X(t) = \left(M_{X0} - \frac{F_S}{m_S}\right) e^{\left(-m_S \cdot Y_{X/S} \cdot (t - t_0)\right)} + \frac{F_S}{m_S} \tag{21}$$

The profile of cumulative CO_2 produced during the fed-batch phase was obtained integrating Eq. (20) using the rectangle rule.

$$M_C(t) = \sum_i \frac{R_C(t_{i-1}) + R_C(t_i)}{2} (t_i - t_{i-1}) \tag{22}$$

Based on reported models for *E. coli*,[16,25] the kinetic parameters used in this model were $Y_{X/S} = 0.69$ Cmol-X · Cmol-S^{-1}, $m_S = 0.024$ Cmol-S · Cmol-X^{-1} · h^{-1}, $Y_{C/S} = 0.26$ Cmol-C · Cmol-S$_{-1}$, and $m_C = 0.02$ Cmol-C · Cmol-X^{-1} · h^{-1}.

The carbon balance was calculated considering the carbon fed into the system $\left(N^{in}_{S,feed}\right)$, the amount of cells produced during the fed-batch phase ($N_{X,ferm} - N_{X,ferm}$ (t_0)), the total amount of CO_2 produced during the fed-batch phase (N_C), and the by-products as total organic carbon in the supernatant ($N_{TOC,sn}$):

$$N_{C,acc} = N^{in}_{S,feed} + N_{X,ferm}(t_0) - N_{X,ferm} - N_C - N_{TOC,sn} \tag{23}$$

$$C - gap(\%) = \frac{N_{C,acc}}{N^{in}_{S,feed}} \cdot 100 \tag{24}$$

4. Results

All experimental profiles of total cell mass (M_x) and the total CO_2 produced (N_{CO2}) followed the trends predicted by the model based on reported kinetic parameters for non-producing *E. coli* under aerobic conditions[16,25] and the experimental feed rates, with an $R^2 > 0.96$ (**Figure 3**) and $R^2 > 0.96$ (results not shown), respectively. Furthermore, the carbon balances closed with less than 5% gap. Profiles of cell mass, dissolved oxygen, CO_2, residual glucose, and typical anaerobic by-products such as ethanol or acetate (results not shown) suggest that there was no oxygen limitation in the vessel. These results indicate that all fermentations were comparable in terms of fermentation performance, independent on whether broth had been circulated through the recovery column (experiments C1–C4) or not (experiments B1–B4). On the other hand, protein levels in the fermentations with both circulation and oil addition (C3 and C4) at the end of the fermentation were, in average, three times higher than in fermentations with oil addition but no circulation (B3 and B4, $p = 0.01 < 0.05$, **Figure 4**A). However, there was no statistically significant difference in viability data ($p = 0.86 > 0.05$) when comparing fermentations with and without circulation through the recovery column (Figure 4B).

Oil hold-up in the top of the column and the percentage of oil recovered indicated a higher degree of coalescence in fermentations without prior circulation to the recovery column (experiments B3 and B4, Figure 5A). However, coalescence into a continuous oil layer could be seen in experiment B4 only. Foam content was considerably higher in fermentations with prior circulation (C3 and C4). This is in agreement with the increased supernatant protein content as seen in Figure 4A and it could indicate a stabilization of gas bubbles by the excess of SACs generated during the fermentation. The resolution of the images did not allow to find significant differences in averaged droplet

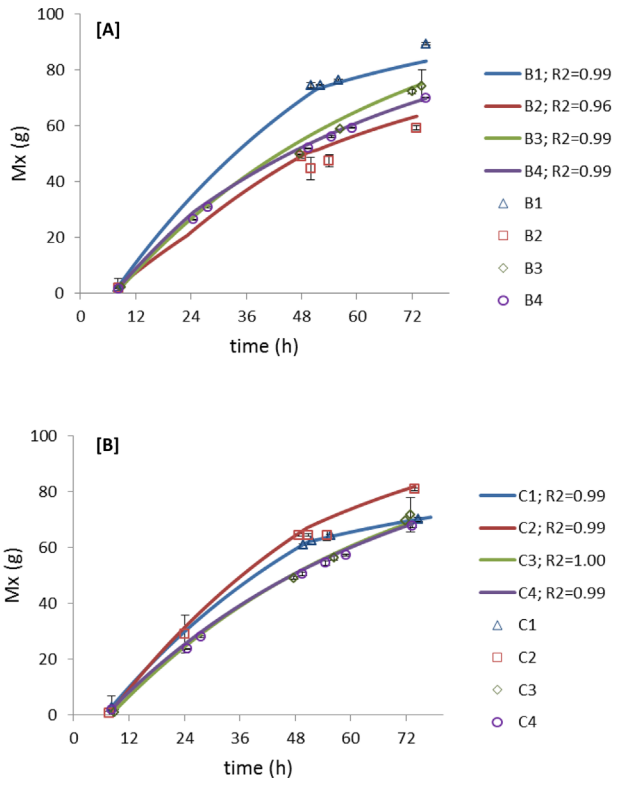

Figure 3. Total mass of cells in the reactor for base case fermentations (A) and circulation case fermentations (B). Solid lines represent data obtained from the kinetic model. Markers represent experimental data obtained from cell dry weight measurements.

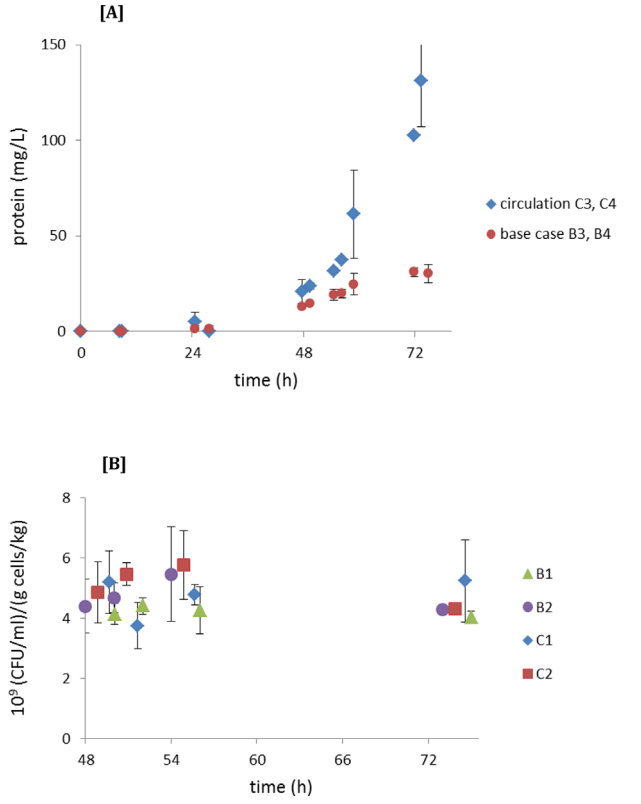

Figure 4. Comparison of base case (B1–B4) and circulation case (C1–C4) based on extracellular protein concentration (A) and cellular viability (B). Error bars represent the standard deviation of the average.

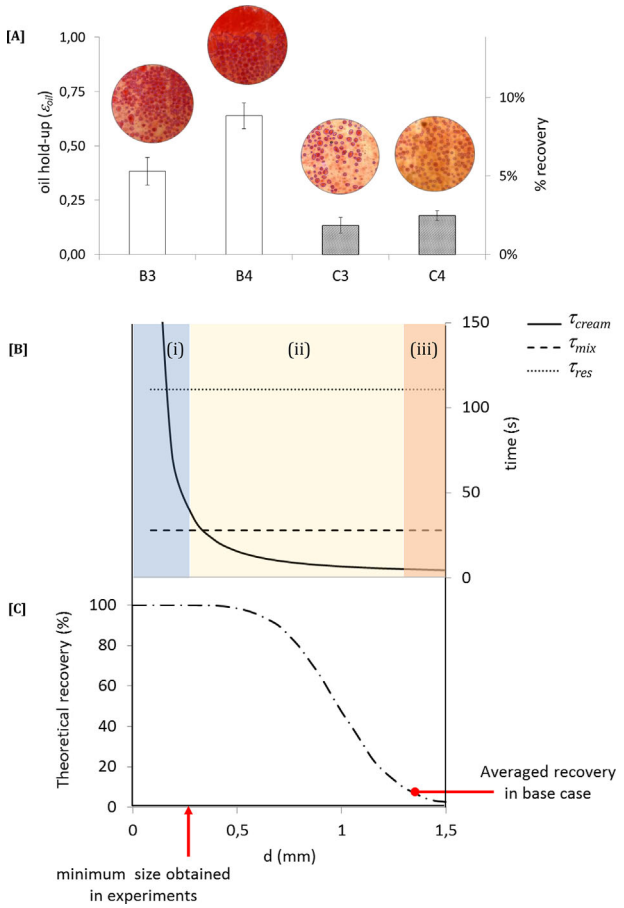

Figure 5. Experimental and theoretical results for oil recovery. A) Experimental results. Bars indicate the significant difference ($p = 0.015 < 0.05$) in oil hold up and percentage of oil recovered between base case (B3, B4) and circulation experiments (C3, C4). Above the bars, pictures of the top of the recovery column for each experiment are shown. B) Comparison of characteristic times as a function of droplet size leading to three regimes in the column (from left to right): (i) circulation of small droplets back to the reactor ($\tau_{res} < \tau_{cream}$), (ii) back-mixing of medium-sized droplets in the column ($\tau_{cream} \sim \tau_{mix}$), (iii) large droplets creaming to the top ($\tau_{cream} << \tau_{mix}$). C) Theoretical recovery as a function of minimum droplet size able to cream ($\tau_{cream} << \tau_{mix}$). Red arrows indicate experimental values.

size between experiments (results not shown). However, oil hold-up was significantly higher ($p = 0.015 < 0.05$) in experiments B3 and B4, at the studied conditions in the GEOR column.

By comparing characteristic times of the main subprocesses (Eqs. (1) and (2)) three different regimes were identified (Figure 5B, from left to right): i) circulation of small droplets back to the reactor when the residence time in the recovery column (τ_{res}) is smaller or in the same order of magnitude than the creaming time (τ_{cream}); ii) medium-sized droplets back-mixed in the column when τ_{res} is an order of magnitude larger than τ_{cream} but the mixing time in the recovery column (τ_{mix}) and τ_{cream} are in the same order of magnitude; iii) large droplets creaming to the top of the column when τ_{mix} is an order of magnitude larger than τ_{cream}. Considering the theoretical droplet size distribution calculated at the bioreactor conditions (see Section 3.5.4), the theoretical recovery as a function of the minimum droplet size able to cream was estimated (see Figure 5C). When comparing the theoretical analysis (Figure 5B and C) to the experimental results (Figure 5A) it can be observed that: a) in all four experiments (B3, B4, C3, and C4) there was creaming, indicating that there were oil droplets of sizes corresponding to regime (iii) in Figure 5B; and b) the percentage of oil recovered in the experiments corresponds to the theoretical recovery for such droplet sizes (Figure 5C). In addition, the minimum droplet size measured in experiments B3, B4, C3, and C4 (0.30 ± 0.04 mm) agreed with the theoretical estimation based on comparison of characteristic times.

5. Discussion

The feasibility of integrating GEOR into a fed-batch fermentation was assessed through kinetic modeling of four integration experiments (B3, B4, C3, and C4) which presented same fermentation performance as four fermentations run without oil recovery (B1, B2, C1, and C2). Duplicates, modeling, and experimental design allowed to systematically study and compare the system with and without circulation through the recovery column, and with and without oil addition. Although circulation through the GEOR column for 24 h at mild mixing and aeration conditions did not affect cell growth or cell viability, it increased the level of SACs in the medium and hindered oil droplet coalescence. The concentration of extracellular proteins in the circulation experiments was up to three times higher than

that of the base case, and most probably have contributed to the emulsion stabilization, as pointed out by Refs. [21,26]. However, further research is needed to determine if other possible SACs like glycolipids from the EPS, or cells with increased hydrophobicity due to stress could have also played a role.[14,15] In any case, it can be stated that from a fermentation perspective it would be desirable to decrease the residence time as much as possible in the circulation loop to reduce the time during which cells are exposed to stress conditions.

The results shown in Figure 5 suggest that stabilization of the oil phase in the form of small droplets decreased the capacity for oil recovery of the GEOR column since small droplets were recirculated back into the vessel or remained back mixed in the column. Estimations based on characteristic times as described in Section 2 indicated that the liquid residence time in the column (111 s) was high enough to retain almost the 100% of the oil fed to the system (Figure 5C). Therefore, according to the estimations, it could be possible to reduce the liquid residence time without significantly reducing the degree of oil recovery. On the other hand, the difference between mixing and creaming time in the column allowed to recover only about 10% v/v of the oil droplets in the top section of the column, while the rest remained back mixed in lower sections (Figure 5). A tuning of the settings in the column is thus required to increase the degree of oil recovery in the GEOR while keeping fermentation performance unaffected. In other words, targeting settings that would lead to a broadening of regime (iii) in Figure 5B. It can be seen that this can be achieved by lowering τ_{cream} and/or increasing τ_{res} and τ_{mix}. In particular, a decrease in aspect ratio would reduce the creaming time (Eq. (5)) increasing the operational window at which oil can be recovered. Clearly, the limit for τ_{res} lies in the stress tolerance and will be microorganism dependent. Although the O_2 transfer in the column could be improved by increasing gas–liquid contact area (e.g., increasing the aeration rate, or reducing the bubble size), these measures might have a negative impact on τ_{mix}. Hence, integration concepts where τ_{res} is minimized are still preferable, for example through novel bioreactor concepts. Furthermore, droplet coalescence and creaming could be promoted by increasing the oil fraction and selecting solvents with lower density (e.g., dodecane). Finally, further studies on the mechanism of oil recovery will allow for more robust design, achieving a compromise between fermentation and recovery requirements in terms of bubble size, number of bubbles, column geometry, residence time, and oil fraction. These studies require improving the acquisition of droplet size data, for example by implementing an in situ optical probe.[27]

From an operational perspective, an in-line GEOR column compared to an off-line separation at the end of the fermentation is more advantageous in cases where long fermentations runs are required (e.g., low productivity, or continuous fermentations). In these cases, prevention of emulsion stabilization over time,[28] or excessive accumulation of oil phase in the bioreactor[11] becomes more relevant. On the other hand, in continuous fermentations the concentration of SACs in the broth is expected to be lower since the medium is continuously refreshed, and therefore the current recovery capacity of the GEOR column could be enough to achieve a formation of a continuous oil phase.

In summary, this study is a step forward in the implementation of GEOR as a feasible in situ product removal technology in multiphase fermentations without affecting fermentation performance in terms of cell growth and cell viability. Further studies with specific microbial systems should be performed to assess the possible effects on product formation. Tuning of GEOR operational parameters is required to improve oil recovery, either by reducing cellular stress conditions or by allowing oil coalescence in an environment with higher concentration SACs. This works consolidates the opportunity for reduction in cost and environmental impact of multiphase fermentations allowing for cell recycle, reducing energy requirements and avoiding the use of chemicals such as surfactants that might compromise product quality.

Abbreviations

CFU, colony-forming unit; DOT, dissolved oxygen tension; GEOR, gas-enhanced oil recovery; SACs, surface active components.

Acknowledgment

This work was carried out within the BE-Basic R&D Program, which was granted a FES subsidy from the Dutch Ministry of Economic affairs.

Conflict of Interest

The authors declare no commercial or financial conflict of interest.

Keywords

emulsion, fermentation, integration, microbial biofuels, product recovery

Received: July 14, 2017
Revised: December 21, 2017
Published online: February 2, 2018

[1] M. A. Rude, A. Schirmer, *Curr. Opin. Microbiol.* **2009**, *12*, 274.
[2] P. Tabur, G. Dorin, (Amyris), *US* 0040396, **2012**.
[3] D. J. McPhee, *Cosm. Toil.* **2014**, *129*, 20.
[4] J. D. Van Hamme, A. Singh, O. P. Ward, *Biotechnol. Adv.* **2006**, *24*, 604.
[5] J. T. Dafoe, A. J. Daugulis, *Biotechnol. Lett.* **2014**, *36*, 443.
[6] J. D. Newman, J. Marshall, M. Chang, F. Nowroozi, E. Paradise, D. Pitera, K. L. Newman, J. D. Keasling, *Biotechnol. Bioeng.* **2006**, *95*, 684.
[7] C. Brandenbusch, B. Bühler, P. Hoffmann, G. Sadowski, A. Schmid, *Biotechnol. Bioeng.* **2010**, *107*, 642.
[8] B. M. Dolman, C. Kaisermann, P. J. Martin, J. B. Winterburn, *Process Biochem.* **2017**, *54*, 162.
[9] J. Kim, E. Iannotti, R. Bajpai, *Biotechnol. Bioprocess Eng.* **1999**, *4*, 1.
[10] A. S. Heeres, J. J. Heijnen, L. A. M. van der Wielen, M. C. Cuellar, *Chem. Eng. Sci.* **2016**, *145*, 31.
[11] K. G. Clarke, L. D. C. Correia, *Biochem. Eng. J.* **2008**, *39*, 405.
[12] A. S. Heeres, *Ph.D. Thesis*, Delft University of Technology, December, **2016**.

[13] D. J. Groen, *Ph.D. Thesis*, Delft University of Technology, October, **1994**.
[14] C. J. Hewitt, G. Nebe-Von Caron, B. Axelsson, C. M. McFarlane, A. W. Nienow, *Biotechnol. Bioeng.* **2000**, *70*, 381.
[15] T. R. Neu, *Microbiol. Rev.* **1996**, *60*, 151.
[16] B. Xu, M. Jahic, S. O. Enfors, *Biotechnol. Prog.* **1999**, *15*, 81.
[17] G. Keitel, U. Onken, *Chem. Eng. Comm.* **1982**, *17*, 85.
[18] A. S. Heeres, C. S. F. Picone, L. A. M. van der Wielen, R. L. Cunha, M. C. Cuellar, *Trends Biotechnol.* **2014**, *32*, 221.
[19] L. S. Dorobantu, A. K. C. Yeung, J. M. Foght, M. R. Gray, *Appl. Environ. Microb.* **2004**, *70*, 6333.
[20] C. Laane, S. Boeren, K. Vos, C. Veeger, *Biotechnol. Bioeng.* **1987**, *30*, 81.
[21] A. S. Heeres, K. Schroen, J. J. Heijnen, L. A. M. van der Wielen, M. C. Cuellar, *Biotechnol. J.* **2015**, *10*, 1206.
[22] C. Verduyn, E. Postma, W. A. Scheffers, J. P. Van Dijken, *Yeast*, **1992**, *8*, 501.
[23] D. J. Korz, U. Rinas, K. Hellmuth, E. A. Sanders, W. D. Deckwer, *J. Biotechnol.* **1995**, *39*, 59.
[24] A. L. Cruz, A. J. Verbon, L. J. Geurink, P. J. Verheijen, J. J. Heijnen, W. M. van Gulik, *Biotechnol. Bioeng.* **2012**, *109*, 1735.
[25] M. C. Cuellar, T. W. Zijlmans, A. J. J. Straathof, J. J. Heijnen, L. A. M. van der Wielen, *Biochem. Eng. J.* **2009**, *44*, 280.
[26] S. Damodaran, *J. Food Sci.* **2005**, *70*, R54.
[27] R. P. Panckow, L. Reinecke, M. C. Cuellar, S. Maaß, *Oil Gas Sci. Technol.* **2017**, *72*, 14.
[28] Z. Kang, A. Yeung, J. M. Foght, M. R. Gray, *Colloids. Surf. B. Biointerfaces* **2008**, *62*, 273.

